

Fabrication and characterization of silver nanostructures using spherical silver nanoparticles released from *Murraya koenigii* leaf extract

Salah Saleh Habtoor^{a,b}, Mohd Arif Agam^{b,*}, Adel Al-Gheethi^{c,*},
Radin Maya Saphira Radin Mohamed^c

^aDepartment of Chemistry and Biology, Faculty of Education, Aden University, Shabwah Branch, Yemen

^bMaterials Physics Laboratory, Faculty of Applied Science and Technology, Bandar Universiti, 84600, Pagoh, Universiti Tun Hussein Onn Malaysia, 84500 Pagoh, Johor, Malaysia, email: arif@uthm.edu.my (M.A. Agam)

^cMicro-pollutant Research Centre (MPRC), Department of Water and Environmental Engineering, Faculty of Civil & Environmental Engineering, Universiti Tun Hussein Onn Malaysia, 86400 Parit Raja, Batu Pahat, Johor, Malaysia, email: adel@uthm.edu.my (A. Al-Gheethi)

Received 16 May 2019; Accepted 29 December 2019

ABSTRACT

Silver nanostructures have gained considerable attention in many applications because of their unique physical and chemical properties such as optical, electronic, surface, shape, and size which are not in bulk material. The most common application is as antimicrobial agents. However, the antimicrobial activity depends on their synthesis process, sizes, and shapes. In the current work, silver nanoparticles (Ag NPs) were synthesized from *Murraya koenigii* leaf extract by a green method using different silver nitrate (AgNO₃) concentrations. The Ag NPs were subjected to the diode laser irradiation (DLI) by using laser radiation at 450 nm wavelengths to change the size and morphology of Ag NPs because this radiation is absorbed in the size of Ag NPs. The formation of Ag NPs was confirmed by the surface plasmon resonance. The Fourier transform-infrared spectroscopy spectra revealed that the presence of biomolecules was responsible for the reduction of silver ions. The field emission scanning electron microscopy showed asymmetric spherical volume of Ag NPs, stable on the leaf extract molecules. Moreover, the Ag NPs modified by DLI exhibited a different change in size and morphology. These findings showed that DLI of silver colloids can aggregate, melt, and fragmentize particles into colloidal nanostructures. The combination of two methods, green synthesis and laser manipulation, gave high productivity. Thus, it can be concluded that the combination of the green synthesis and laser manipulation in liquids can fabricate nanoparticles of different shapes and sizes, and characterized for efficiency as antimicrobial agents.

Keywords: Silver nanoparticles; Nanostructures; Diode laser; Characterization

1. Introduction

Metallic nanoparticles are of great importance in many fields and applications such as medicine and electronics. This is because they have unique optical, electronic, chemical, and physical properties, and can be applied in drug delivery, catalysis, and sensing [1]. The morphological and

crystalline properties of nanostructure made them distinctive. Therefore, researchers are looking for ways which might produce and control the shapes and sizes of nanoparticles [2]. Many methods are available for the production of silver nanoparticles (Ag NPs) such as thermal decomposition [3], chemical reactions [4], electrochemical [5], and microwave-assisted process [6]. The development of chemical

* Corresponding authors.

and physical techniques in the production of nanomaterials is associated with the concern over environmental pollution because the use of chemical and physical methods generate hazardous secondary waste [7]. Therefore, a safe, non-toxic, clean, and environmentally friendly way to produce nanoparticles is needed. As a result, researchers have led to biochemical systems in the production of nanoparticles. Bio-synthesis methods have paved the way for the “green chemistry” of nanoparticles.

The use of environmentally friendly materials such as plant extracts, fungi, bacteria, enzymes to produce Ag NPs offers many benefits that are compatible with biomedical and pharmaceutical applications [8]. It has been demonstrated that green synthesis is better than chemical and physical methods because it is efficient, cost-effective, environmentally friendly and safe for medical use [9]. It is possible to increase the production process easily on a wider scale. This technique also does not require high temperature or high pressure or toxic chemicals. Recently, *Murraya koenigii* leaves were reported to have antioxidant properties due to the presence of highly concentrated carbazole compounds [10], which play a major role in reducing and stabilizing metal ions. The reduction of silver ions into Ag NPs using *M. koenigii* leaf extract has prompted expansion on the research to produce Ag NPs impregnated microcrystalline cellulose as filler material. A curative result from *M. koenigii* extract was observed in the reduction of silver ions into nanoparticles. Many literatures reported on the rapid synthesis of gold and Ag NPs from *M. koenigii* leaves extract [11]. However, studies conducted on the synthesis of colloidal nanostructures of Ag NPs from *M. koenigii* are very few. Pumped laser irradiation in liquid media has become an increasingly important alternative approach to produce colloidal nanostructures with new functional properties [12]. The properties of Ag NPs including their magnetic properties and surface plasmon resonance (SPR) sensors can be useful for their applications in stimulation, information storage, electronic optics, sensors, and biofuel technology [13]. Despite the multiple advantages of laser in the production of nanostructures, it has the problem of low productivity [14]. Characterization for efficiency, simplicity, and high productivity demonstrates the mechanism of laser irradiation to modify the nanoparticles. It is necessary to obtain optimal conditions and control the process.

The idea in the current work is based on the modification of Ag NPs, where the nanoparticles have a resonant absorption of the SPR in a visible spectrum [15]. Nanoparticles were produced as the first step by the prevailing mechanism of biosynthesis as an adaptation of the so-called green synthesis. These nanoparticles were subjected to a wavelength laser close to the SPR peak of Ag NPs to form nanoparticles with different sizes and shapes. The laser excites through two mechanisms to aggregate and to fragment the size of the particle [16,17]. In this work, diode laser irradiation (DLI) pumped green synthesized Ag NPs colloids at wavelength 450 nm to release the spherical Ag NPs plant leaf and modify the shape and the size of the nanoparticle. More details are required to expand the *M. koenigii* reduction mechanism for different applications. Due to the lack of qualitative and quantitative data on the various Ag NPs using biological systems, this study aims to synthesis Ag NPs with aqueous

extract of *M. koenigii* leaves at different concentrations of silver salts, to fabricate colloidal silver nanostructures via DLI, and to characterize Ag NPs and nanostructures using Fourier transform-infrared spectroscopy (FTIR), field emission scanning electron microscopy (FESEM), ultraviolet-visible (UV-Vis) spectroscopy, X-ray diffraction (XRD), and atomic force microscope (AFM).

2. Materials and methods

2.1. Preparation of silver nitrate solution

The silver nitrate (AgNO_3) solution was prepared by dissolving 16.9, 50.9, and 84.9 mg of NaNO_3 in 100 mL of distilled water to prepare 1, 3, and 5 mM, respectively.

2.2. Preparation of the plant extract

The plant extract was prepared by using 10 g of fresh plant leaves bought from the local supermarket in Johor, Malaysia. The leaves were washed thoroughly three times with distilled water to remove unwanted particles. The leaves were cut into small pieces and then placed in a 300 mL beaker containing 100 mL distilled water, boiled at 90°C for 15 min. The solution was cooled at room temperature and then filtered by filter paper Whatman No.1. Pure solution was stored at 4°C until further use [18].

2.3. Synthesis of silver nanoparticles

A fixed volume (100 mL) of AgNO_3 solutions (at different concentrations, 1, 3, and 5 mM) was transferred into separate flasks (250 mL). The plant extract (2 mL) was added into each flask. The mixture was left at room temperature overnight. The color of the mixture changed from colorless to yellow within the first minute of the reaction, indicating the beginning of the Ag NPs formation, after 2 h the color changed to brown, and the color changed into dark brown after overnight indicating the formation of silver particles. Ag NPs were separated from the mixture by centrifugation at 13,000 rpm for 30 min, suspended with deionized water, and then kept in a small tube for analysis.

2.4. Fabrication of silver nanostructures

The synthesized nanoparticles were irradiated by the DLI system at 450 nm wavelength with a maximum energy of 2,000 mW. The particles were released from the plant leaf and manipulated using laser diode irradiation to obtain colloid silver nanostructure with different optical, chemical, and physical properties. The characteristics of the colloidal solution were determined using UV-Visible spectroscopy and FESEM microscopy. Ag NPs have been irradiated via laser beams without using focus. Moreover, the Ag NPs were exposed to 1,100 mW laser irradiation energy for 1 min to release spherical Ag NPs from the plant leaf followed by exposure at different times for 10, 15, and 20 min to obtain nanostructures. The characterization via UV-Visible spectroscopy was made after every irradiation exposure and FESEM. The immersed clean glass plate was fixed on a scale of 2 × 2 cm with the Ag NPs solution and dried to be analyzed using XDR.

2.5. Characterization of Ag NPs and nanostructures

Ag NPs was confirmed using UV-Vis spectrophotometer after 48 h. Ag NPs have free electrons on their surface that are responsible for the absorption of SPR in the ultraviolet spectrum. The UV-vis spectrum showed a peak due to the interaction of free electrons on the surface of the metal nanoparticles with specific wavelengths. The silver ions were reduced; this process was confirmed by UV-Vis spectroscopy in the region between 400 and 450 nm. FTIR was used to determine the functional groups associated with the prepared metallic nanoparticles. The crystalline nature of the green synthesized Ag NPs was confirmed from the XRD patterns. Characterization of FESEM was also used to study the morphological surface and the size of metallic nanoparticles. AFM images were used to quantify the topography of and the surface roughness of nanoparticles.

2.6. Antibacterial activity of Ag NPs

In order to investigate the applicability of the Ag NPs synthesized in the present study, the antimicrobial properties of Ag NPs against *Escherichia coli* and *Staphylococcus aureus* were studied. The test was conducted on Müller-Hinton agar using agar diffusion assay at three concentrations of Ag NPs (1, 5, and 10 μL) according to Noman et al. [19].

3. Results and discussions

3.1. UV-Vis absorption spectra of Ag NPs and nanostructure

The results for the UV-Vis spectrophotometer of the Ag NPs prepared in the current work are presented in Fig. 1a. The peaks are shown at 426, 435, and 441 nm for the three types of silver solutions investigated (1, 3, and 5 mM). The high peak appeared at 441 nm, indicating the high amount of nanoparticles. Similar results was also reported by [20], who prepared Ag NPs from *Tephrosia purpurea* leaf extract [21].

The appearance of the absorption peak indicates the conversion of silver ions into nanoparticles [22]. The spherical Ag NPs peaks after laser irradiation at 1, 10, 15, and 20 min are respectively shown at 404, 381, 411, and 439 nm (Fig. 1b). These findings showed that SPR peak absorption center was converted toward a shorter wavelength. The changes in the UV-Vis spectrum indicate that the dimension of particle and size distribution were decreased through laser radiation. Obviously, the premier UV-Vis spectrum was changed by laser beams. The plasmon resonance bandwidth is greatly reduced indicating the reduction of Ag NPs particle size [23]. The change in the plasmon wavelength was accompanied by an increase in absorption. Since the frequency of plasmon for each particle is specified by its shape and dimension, the optical absorption of particle distributions are homogeneously displayed. Therefore, irradiation of nanoparticles in liquid with a laser beam of specified photon power produces SPR in particles with specific shape and size.

3.2. Fourier infrared spectra and XRD of Ag NPs

The FTIR spectra of Ag NPs prepared from the *M. koenigii* leaf extract are shown in Fig. 2. The results showed the existence of different functional groups including alkane, alkene, methylene groups, carboxylic acids, and amine groups. These functional groups have potential as a reducing agent in Ag NPs synthesis. These peaks indicate the presence of a carbonyl group that forms the amino acid residues which capped Ag nanoparticles to prevent aggregation, thus stabilizing the medium [24]. The peaks at $1,620\text{--}1,636\text{ cm}^{-1}$ indicate the presence of carbonyl groups of polyphenols such as epicatechin gallate, epigallocatechin, catechin gallate, galocatechin gallate, theaflavin, and epigallocatechin gallate. These findings indicate that the molecules are attached with Ag NPs. The amide groups might exist in the aromatic rings. This concludes that the polyphenol compounds attached to the Ag NPs could be bound with the amide region and an

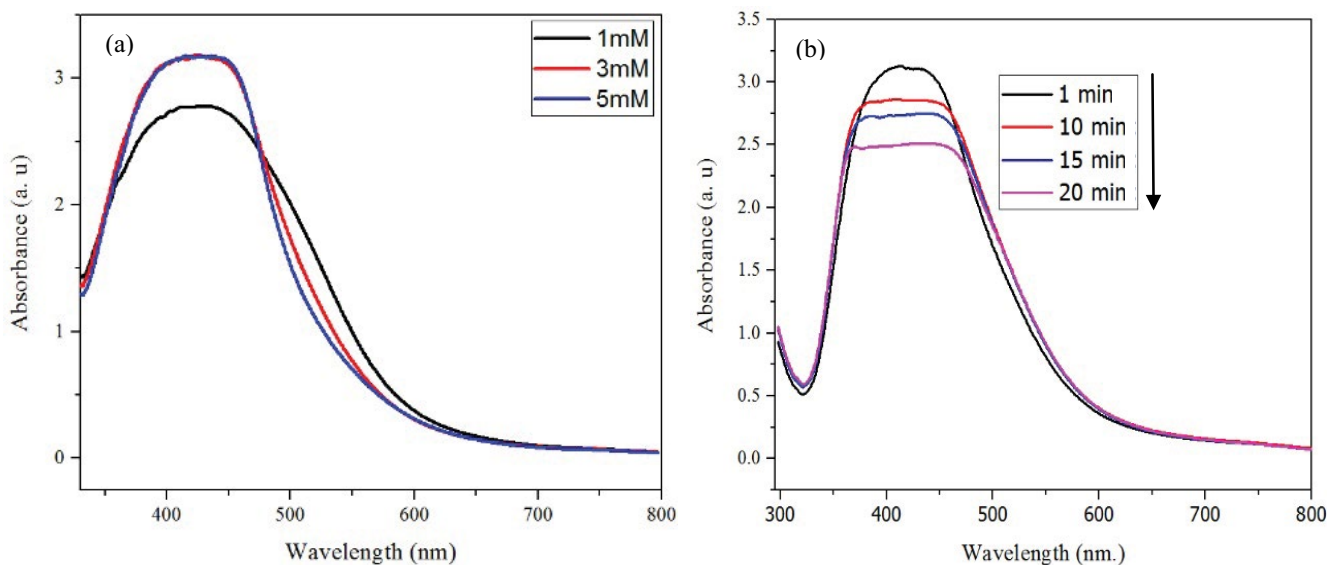


Fig. 1. UV-Vis spectra of colloid Ag NPs. (a) AgNPs by *M. Koenigii* leaf extract with AgNO_3 solutions and (b) Ag NPs after laser irradiation 1,100 mW at different times.

aromatic ring [25]. The strong and broad peak at $3,326.13\text{ cm}^{-1}$ confirms the OH stretching that indicates the presence of alcohols or carboxylic acids. The crystalline nature of Ag NPs was confirmed by XRD analysis (Fig. 3). The main peaks of XRD analysis were observed at 38.1° , 44.3° , 64.5° , 77.4° , and 81.5° . These peaks are corresponding to (1 1 1), (2 0 0), (2 2 0), (3 1 1), and (2 2 2) planes of the face-centered cubic structure of Ag NPs (JCPDS) file: No. 04-0783. The undetermined peaks at $2\theta = 27.9^\circ$ and 32.2° indicated by (*) are attached to crystalline organic phases. The crystalline size and full width at half

maximum (FWHM) parameters of the synthesized Ag NPs samples Ag-1, Ag-3, and Ag-5 with different concentrations (1, 3, and 5 mM) are shown to be accompanied by each sample (Table 1). This is also in agreement with several reports on XRD patterns of the green synthesized Ag NPs [26].

3.3. Surface morphology of Ag NPs

Surface morphology of the nanoparticles was obtained from FESEM analysis. Fig. 4 shows FESEM and EDS

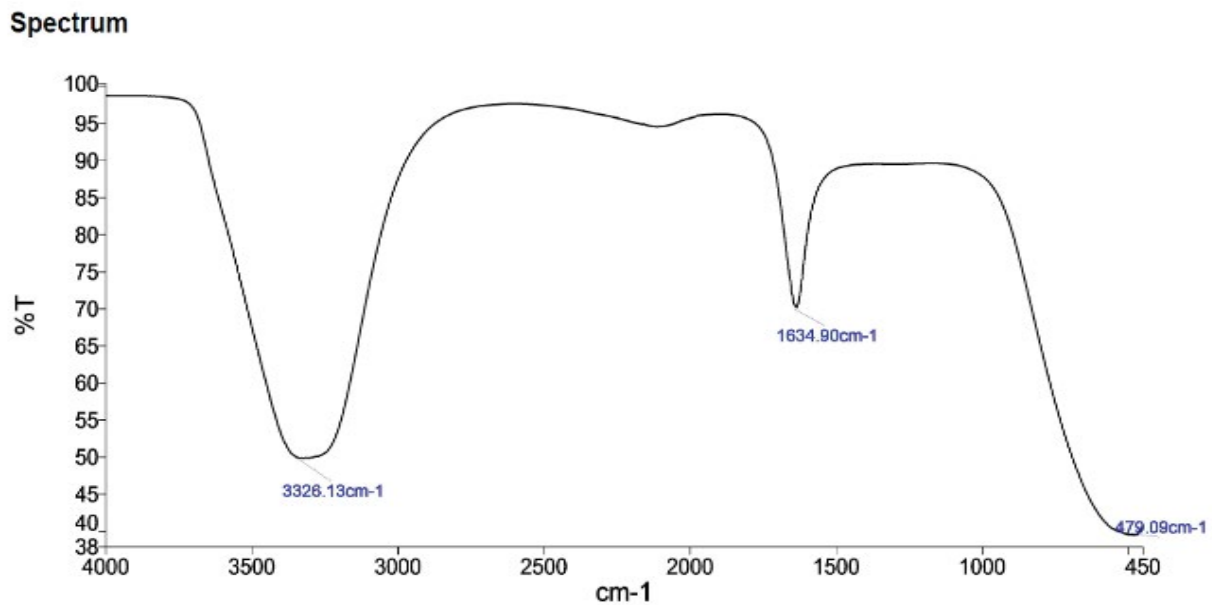


Fig. 2. FTIR spectroscopy of Ag nanoparticles synthesized by extract of *M. koenigii* leaf.

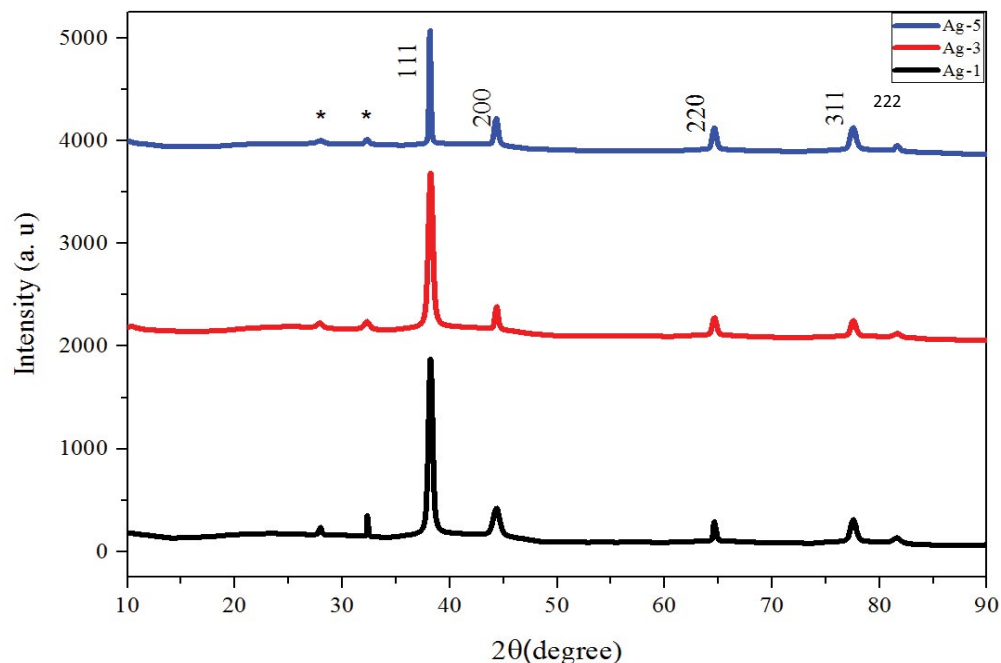


Fig. 3. XRD pattern of silver nanoparticles synthesized using treating AgNO_3 with *M. Keonigii* leaf extract.

Table 1
Represents of structural parameters for synthesized silver nanoparticles

Samples	2 θ (°)	FWHM	Crystalline size (Å)
Ag-1	38.211	0.4330	2.35537
Ag-3	38.219	0.4723	2.35489
Ag-5	38.163	0.1378	2.35821

analysis of Ag NPs synthesized with different concentrations of AgNO₃. The attachment of energy-dispersive X-ray spectroscopy (EDS) current with the FESEM was known to provide information on the chemical analyses of the areas being searched or the structure at spot EDS. The results revealed that more Ag NPs were synthesized with 5 mM of AgNO₃ solution. Moreover, the surface morphology of Ag NPs, and their shape and arrangements were released after exposure to the laser irradiation. The majority consisted of roughly

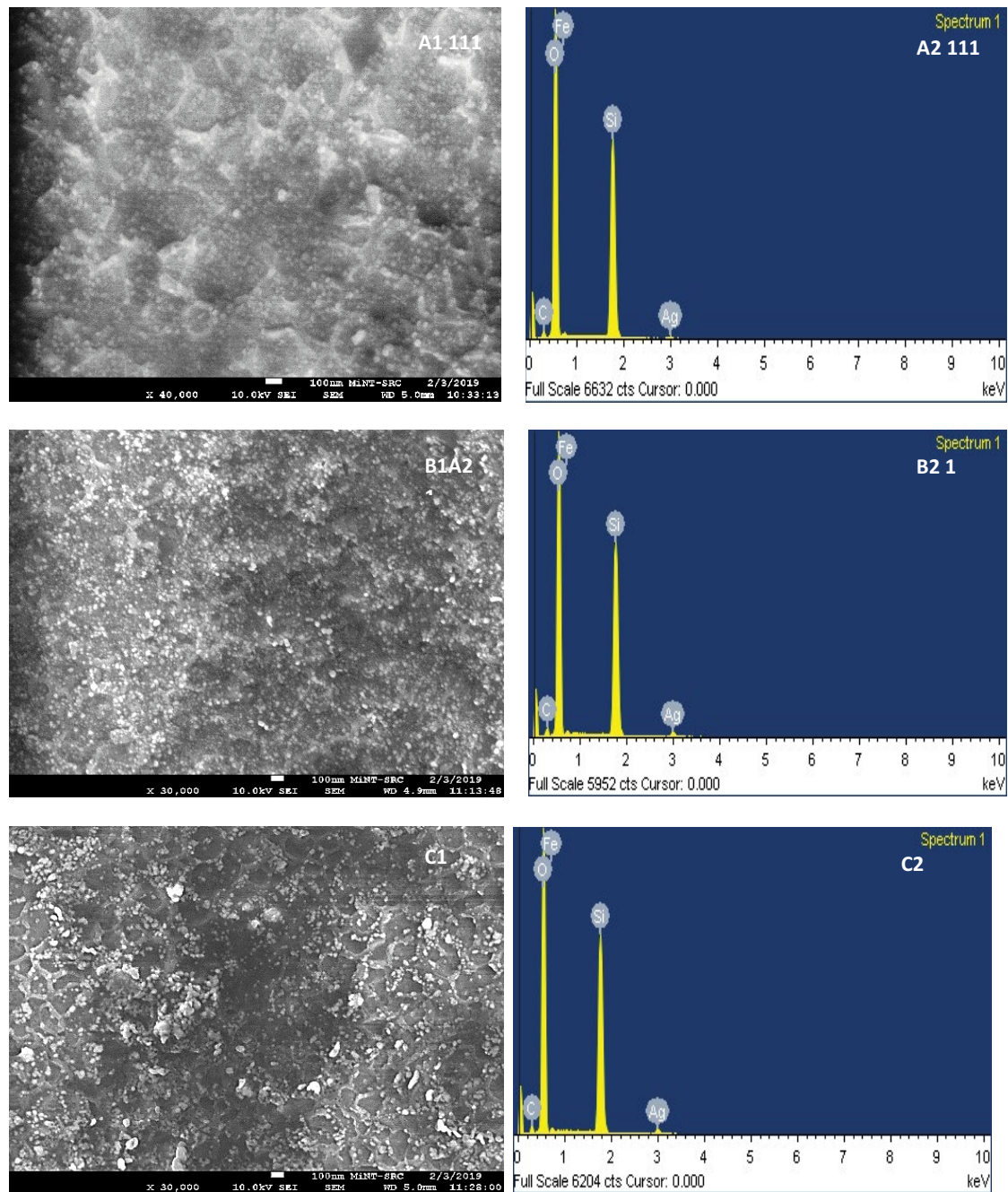


Fig. 4. FESEM of Ag NPs synthesized from *M. koenigi* leaf extract. (a1) FESEM of Ag NPs synthesized with 1 mM of AgNO₃, (b1) FESEM of Ag NPs synthesized with 3 mM of AgNO₃, (c1) FESEM of Ag NPs synthesized with 5 mM of AgNO₃, (a2) Elemental analysis by EDS of Ag NPs synthesized with 1 mM of AgNO₃, (b2) EDS of Ag NPs synthesized with 3 mM of AgNO₃, and (c2) EDS of Ag NPs synthesized with 5 mM of AgNO₃.

spherical particles of Ag NPs. These nanoparticles show a slight tendency to aggregate, melt, and fragmentize over time (Fig. 5).

The AFM analysis of Ag NPs synthesized from 1 mM of AgNO_3 showed that the particles' surface has tips and scattered nanoparticles, the 3D image displays that the nanoparticles have sharp tips of nails on the extracted

surface (Figs. 6a1 and a2). The Ag NPs synthesized from 3 mM of AgNO_3 showed a scattered nanoparticle and tips on the surface (Fig. 6b1). In contrast, the nails of nanoparticles with tips have sharp shapes on the extracted surface (Fig. 6b2). The Ag NPs synthesized from 5 mM of AgNO_3 covered surface are closely packed with groups of nanoparticles (Fig. 6c1), while the 3D image shows a sharp

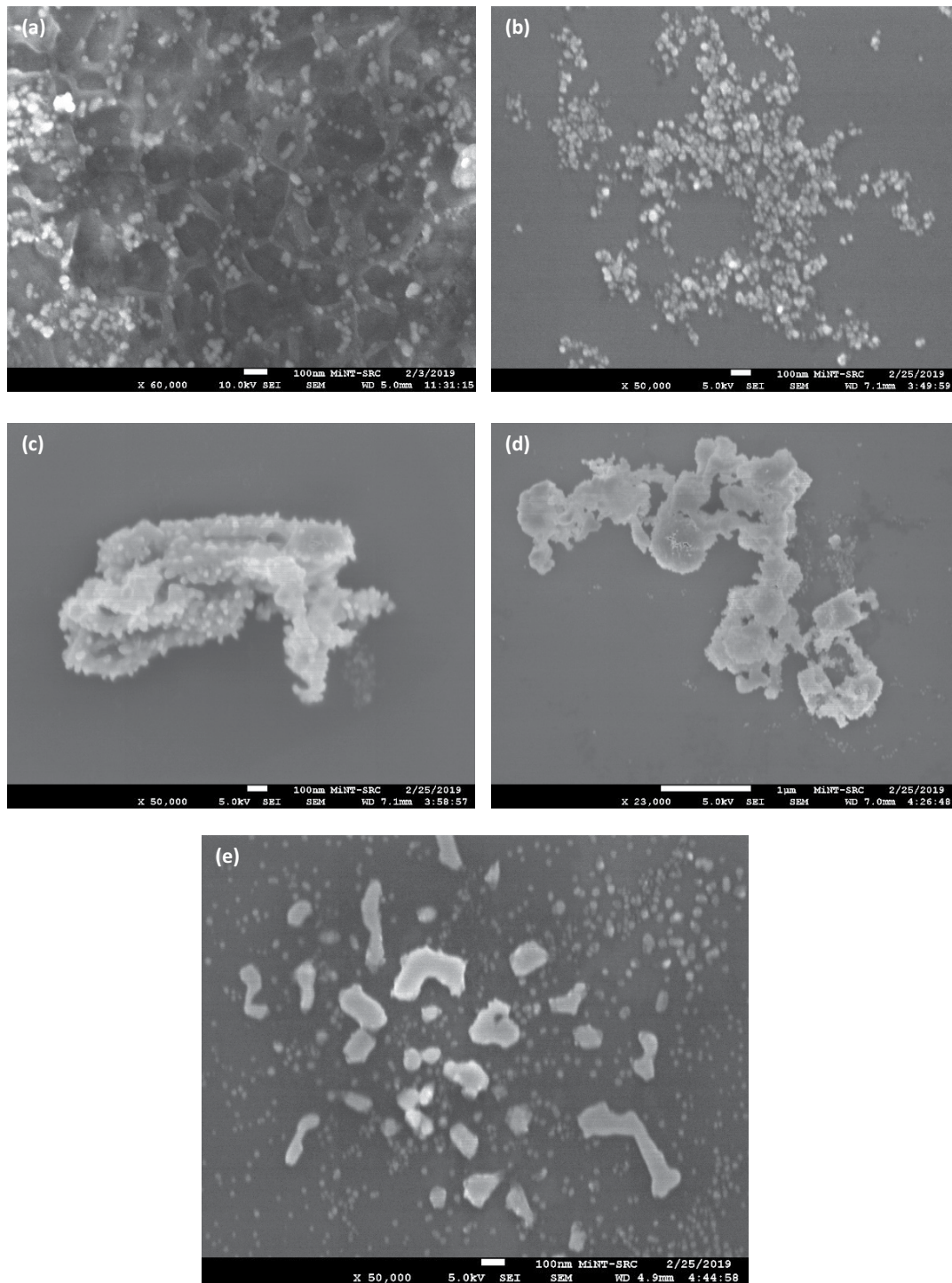


Fig. 5. Images of FESEM of unirradiated (a) and irradiated Ag NPs, (b) the released spherical silver NPs for 1 min, (c) the released spherical silver NPs for 10 min, (d) the released spherical silver NPs for 15 min, and (e) the released spherical silver NPs for 20 min.

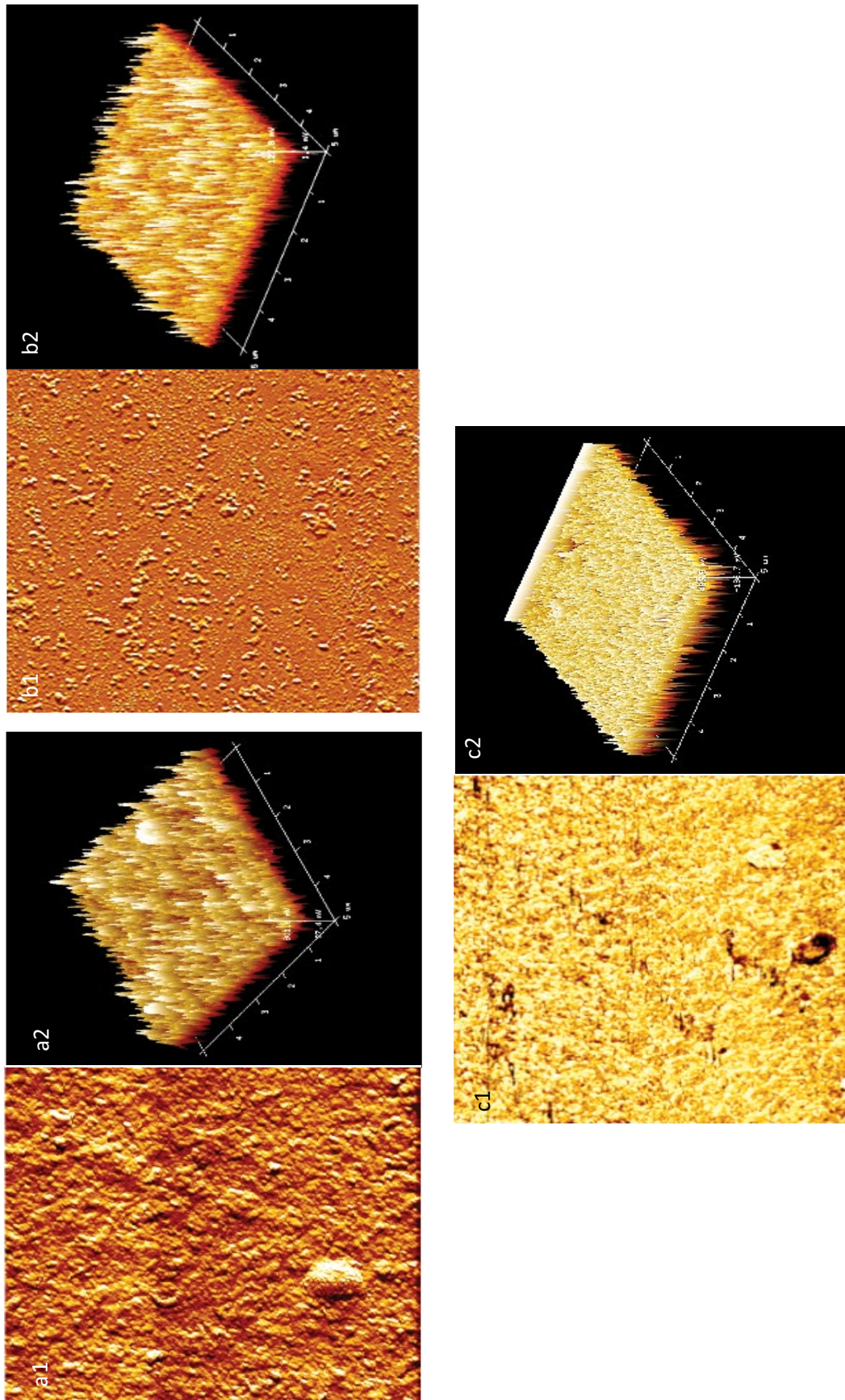


Fig. 6. AFM analysis of Ag NPs. (a1 and a2) 2D and 3D of Ag NPs synthesized from 1 mM of AgNO_3 , (b1 and b2) 2D and 3D of Ag NPs synthesized from 3 mM of AgNO_3 , and (c1 and c2) 2D and 3D of Ag NPs synthesized from 5 mM of AgNO_3 .

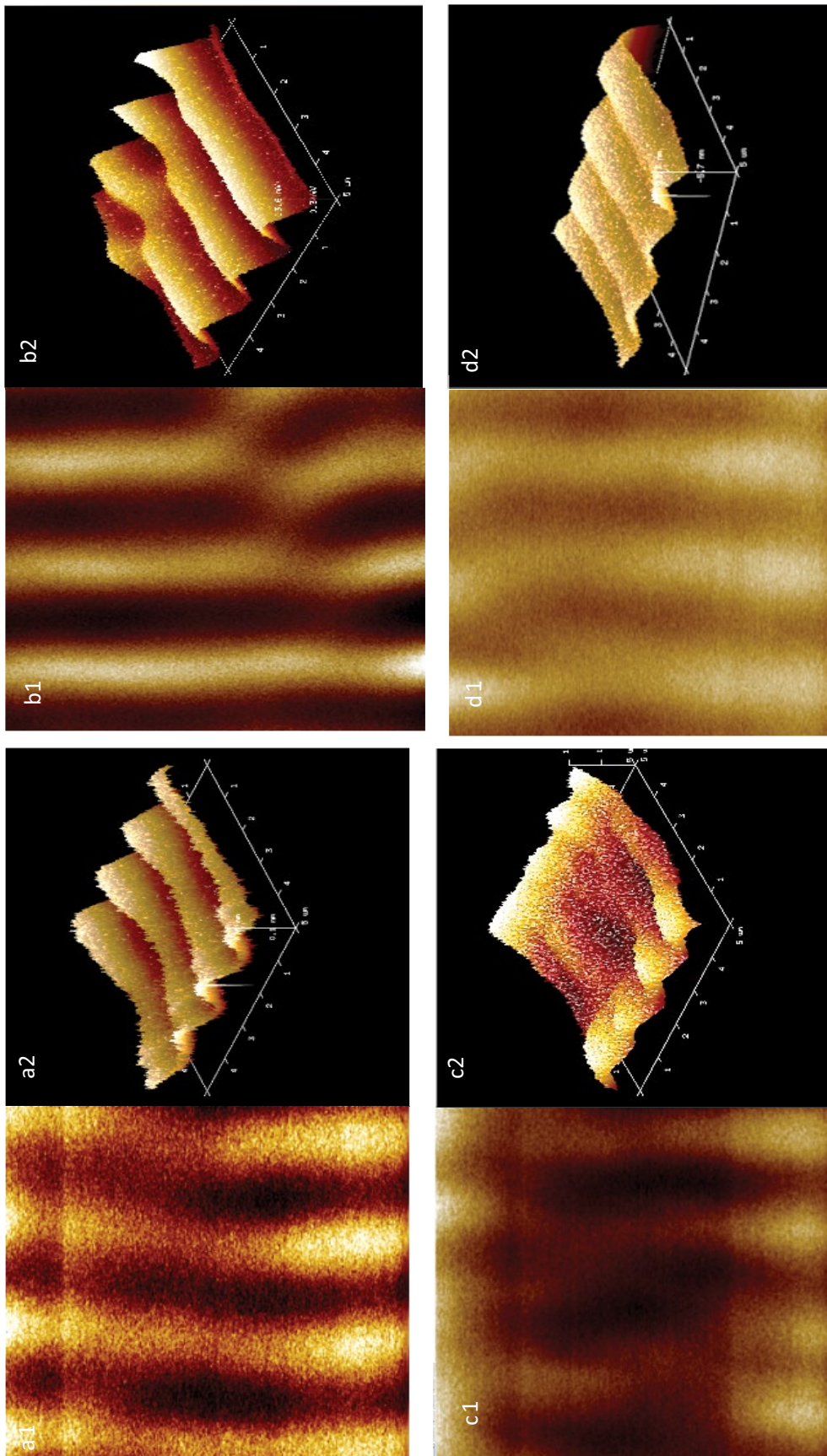


Fig. 7. AFM analysis of Ag nanostructure after exposure for the laser irradiation. (a1 and a2) 2D and 3D of Ag NPs synthesized from 5 mM of AgNO_3 (untreated), (b1 and b2) 2D and 3D of Ag NPs after laser irradiation for 15 min, and (c1 and c2) 2D and 3D of Ag NPs after laser irradiation for 10 min, and (d1 and d2) 2D and 3D of Ag NPs after laser irradiation for 20 min.

Table 2
Antibacterial activity of Ag NPs against *E. coli* and *S. aureus*

Bacteria strain	<i>E. coli</i>			<i>S. aureus</i>		
Ag NPs (μL)	1	5	10	1	5	10
Inhibition zone (mm)	9	12	18	10	13	15

nanoparticles pointer on the surface (Fig. 6c2). The cracks and pits observed in the AFM image of the samples remain on the glass substrate due to the impact and high capacity ions that shot the substrate [27]. On the surface, agglomerates and particle distribution may occur when nanoparticles tend to contact together rather than stuck with the substrate [28]. AFM analysis of Ag NPs after laser irradiation is shown in 2D and 3D in Figs. 7a1–d2. The AFM images display that some Ag NPs might change their shape to different nanostructures, and some nanoparticles are still visual.

3.4. Antibacterial activity of Ag NPs

Ag NPs synthesized by *M. koenigii* revealed antibacterial activity against *E. coli* and *S. aureus*. The inhibition zone was between 9 and 18 mm for *E. coli* and between 10 and 15 mm for *S. aureus* (Table 2). These results confirmed that applicability of Ag NPs for disinfection of water and wastewater. In comparison, revealed that Ag NPs from *Aspergillus iizukae* EAN605 exhibited antimicrobial activity against *E. coli* and *S. aureus* [29]. However, the antimicrobial activity recorded here exhibited more inhibition efficiency. These findings indicated that the Ag NPs from *M. koenigii* has the potential to be used for the disinfection of wastewater and inactivation of pathogenic bacteria.

4. Conclusions

The present study concluded that the UV-Visible spectroscopy clearly showed three peaks for Ag NPs based on the initial concentration of AgNO_3 used in the synthesis process. Moreover, the changes in the UV-Visible spectra after laser irradiation were showed to correspond to aggregation, melting, and fragmentation of the particles in the solution. The formation of Ag NPs was confirmed through the FTIR study, which confirmed the emergence of different functional groups for different types of phytochemicals. It can be concluded that Ag NPs formed because of the reduction and stability of agents in the *M. koenigii* leaf extract. The combination of both green synthesis and laser manipulation techniques in liquid create the different shape of nanostructures. The prepared nanostructures by this combined method gave a height purity since there is no existence of chemicals in the synthesis of particle. The antimicrobial test confirms the ability of Ag NPs to inactivate the pathogenic bacteria and indicate the applicability of Ag NPs for water and wastewater treatment.

Acknowledgment

The authors appreciate the support from the Ministry of Education, Malaysia through FRGS Vot. K090 and Universiti

Tun Hussein Onn under GPPS grant Vot. U777 that greatly assisted the research.

References

- [1] D. Vilela, M.C. González, A. Escarpa, Sensing colorimetric approaches based on gold and silver nanoparticles aggregation: chemical creativity behind the assay. A review, *Anal. Chim. Acta*, 751 (2012) 24–43.
- [2] K. An, G.A. Somorjai, Size and shape control of metal nanoparticles for reaction selectivity in catalysis, *ChemCatChem*, 4 (2012) 1512–1524.
- [3] S.M. Hosseinpour-Mashkani, M. Ramezani, Silver and silver oxide nanoparticles: synthesis and characterization by thermal decomposition, *Mater. Lett.*, 130 (2014) 259–262.
- [4] J. García-Barrasa, J.M. López-de-Luzuriaga, M. Monge, Silver nanoparticles: synthesis through chemical methods in solution and biomedical applications, *Cent. Eur. J. Chem.*, 9 (2011) 7–19.
- [5] R.A. Khaydarov, R.R. Khaydarov, O. Gapurova, Y. Estrin, T. Scheper, Electrochemical method for the synthesis of silver nanoparticles, *J. Nanopart. Res.*, 11 (2009) 1193–1200.
- [6] H. Peng, A. Yang, J. Xiong, Green, microwave-assisted synthesis of silver nanoparticles using bamboo hemicelluloses and glucose in an aqueous medium, *Carbohydr. Polym.*, 91 (2013) 348–355.
- [7] S. Ahmed, S. Ikram, Synthesis of gold nanoparticles using plant extract: an overview, *Nano Res. Appl.*, 1 (2015) 1–6.
- [8] S. Vijayakumar, B. Vaseeharan, B. Malaikozhundan, M. Shobiya, *Laurus nobilis* leaf extract mediated green synthesis of ZnO nanoparticles: characterization and biomedical applications, *Biomed. Pharmacother.*, 84 (2016) 1213–1222.
- [9] S. Iravani, H. Korbekandi, S.V. Mirmohammadi, B. Zolfaghari, Synthesis of silver nanoparticles: chemical, physical and biological methods, *Res. Pharmacol. Sci.*, 9 (2014) 385.
- [10] L.J.M. Rao, K. Ramalakshmi, B.B. Borse, B. Raghavan, Antioxidant and radical-scavenging carbazole alkaloids from the oleoresin of curry leaf (*Murraya koenigii Spreng.*), *Food Chem.*, 100 (2007) 742–747.
- [11] F.A. Qais, A. Shafiq, H.M. Khan, F.M. Husain, R.A. Khan, B. Alenazi, A. Alsalmeh, I. Ahmad, Antibacterial effect of silver nanoparticles synthesized using *Murraya koenigii* (L.) against multidrug-resistant pathogens, *Bioinorg. Chem. Appl.*, 2019 (2019), doi: 10.1155/2019/4649506.
- [12] Y. Wang, H. Sun, Advances and prospects of lasers developed from colloidal semiconductor nanostructures, *Prog. Quantum Electron.*, 60 (2018) 1–29.
- [13] M. Rafique, I. Sadaf, M.S. Rafique, M.B. Tahir, A review on green synthesis of silver nanoparticles and their applications, *Artif. Cells Nanomed. Biotechnol.*, 45 (2017) 1272–1291.
- [14] S. Kadhem, H. Humud, I.M. Abdulmajeed, Silver nanofluids prepared by pulse exploding wire, 1 (2014) 317–327.
- [15] A. Moores, F. Goettmann, The plasmon band in noble metal nanoparticles: an introduction to theory and applications, *New J. Chem.*, 30 (2006) 1121–1132.
- [16] G. Guisbiers, Q. Wang, E. Khachatryan, M.J. Arellano-Jimenez, T.J. Webster, P. Larese-Casanova, K.L. Nash, Anti-bacterial selenium nanoparticles produced by UV/VIS/NIR pulsed nanosecond laser ablation in liquids, *Laser Phys. Lett.*, 12 (2014) 16003.
- [17] N.V. Tarasenko, A.V. Butsen, E.A. Nevar, Laser-induced modification of metal nanoparticles formed by laser ablation technique in liquids, *Appl. Surf. Sci.*, 247 (2005) 418–422.
- [18] J.L. Gardea-Torresdey, E. Gomez, J.R. Peralta-Videa, J.G. Parsons, H. Troiani, M. Jose-Yacaman, Alfalfa sprouts: a natural source for the synthesis of silver nanoparticles, *Langmuir*, 19 (2003) 1357–1361.
- [19] E. Noman, A. Al-Gheethi, B. Talip, R. Mohamed, R.A. Kassim, Inactivating pathogenic bacteria in greywater by biosynthesized Cu/Zn nanoparticles from secondary metabolite of *Aspergillus iizukae*; optimization, mechanism and techno economic analysis, *PloS one*, 14 (2019) e0221522.
- [20] R. Vijayan, S. Joseph, B. Mathew, Green synthesis, characterization and applications of noble metal nanoparticles

- using *Myxopyrum serratum* AW Hill leaf extract, *Bionano-science*, 8 (2018) 105–117.
- [21] B. Ajitha, Y.A.K. Reddy, P.S. Reddy, Biogenic nano-scale silver particles by *Tephrosia purpurea* leaf extract and their inborn antimicrobial activity, *Spectrochim. Acta, Part A*, 121 (2014) 164–172.
- [22] M.R. Bindhu, M. Umadevi, Antibacterial and catalytic activities of green synthesized silver nanoparticles, *Spectrochim. Acta, Part A*, 135 (2015) 373–378.
- [23] K.-S. Lee, M.A. El-Sayed, Gold and silver nanoparticles in sensing and imaging: sensitivity of plasmon response to size, shape, and metal composition, *J. Phys. Chem. B*, 110 (2006) 19220–19225.
- [24] R. Sathyavathi, M.B. Krishna, S.V. Rao, R. Saritha, D.N. Rao, Biosynthesis of silver nanoparticles using *Coriandrum sativum* leaf extract and their application in nonlinear optics, *Adv. Sci. Lett.*, 3 (2010) 138–143.
- [25] V. Kumar, S.C. Yadav, S.K. Yadav, *Syzygium cumini* leaf and seed extract mediated biosynthesis of silver nanoparticles and their characterization, *J. Chem. Technol. Biotechnol.*, 85 (2010) 1301–1309.
- [26] D. Philip, C. Unni, S.A. Aromal, V.K. Vidhu, *Murraya koenigii* leaf-assisted rapid green synthesis of silver and gold nanoparticles, *Spectrochim. Acta, Part A*, 78 (2011) 899–904.
- [27] Y. Malhotra, M.P. Srivastava, AFM, XRD and optical studies of silver nanostructures fabricated under extreme plasma conditions, *J. Phys.: Conf. Ser.*, 511 (2014) 12072.
- [28] B.B. Borse, L.J.M. Rao, K. Ramalakshmi, B. Raghavan, Chemical composition of volatiles from coconut sap (neera) and effect of processing, *Food Chem.*, 101 (2007) 877–880.
- [29] C. Baker, A. Pradhan, L. Pakstis, D.J. Pochan, S.I. Shah, Synthesis and antibacterial properties of silver nanoparticles, *J. Nanosci. Nanotechnol.*, 5 (2005) 244–249.